A Boolean Lattice Gas Method for Predicting Intrinsic Permeability of Porous Media.

L.O. E. Santos[1], P.C. Philippi[2]•, M.C. Damiani[3]

(+) Porous Media and Thermophysical Properties Laboratory (LMPT).
Mechanical Engineering Department. Federal University of Santa Catarina
88040-900 Florianópolis, SC, Brazil.
(*) Engineering Simulation and Scientific Software (ESSS)
Parque Tecnológico de Florianópolis - Rodovia SC 401 km 001
88030-000 Florianópolis , SC, Brasil

Abstract

This paper presents a method for predicting intrinsic permeability of porous media based on Lattice Gas Cellular Automata (LGA) methods. LGA is a relatively recent method developed to perform hydrodynamic calculations. The method, in its simplest form, consists of a regular lattice populated with particles that hop from site to site in discrete time steps in a process, called *propagation*. After propagation, the particles in each site interact with each other in a process called *collision*, in which the number of particles and momentum are conserved. An exclusion principle is imposed in order to achieve better computational efficiency. In despite of its simplicity, this model evolves in agreement with Navier-Stokes equation for low Mach numbers. It is important to emphasize some aspects that make LGA methods very attractive for simulating flows through porous media. In fact, boundary conditions in flows through complex geometry structures are very easy to describe in LG simulation. Simulations are performed with integers needing less resident memory capability and boolean arithmetic reduces running time. The method is used to simulate flows through several Brazilian reservoir petroleum rocks leading to intrinsic permeability prediction. Simulation is compared with experimental results.

Keywords: *fluid flow, porous media, permeability, lattice-gas*

---

[1] *Luis Orlando Emerich dos Santos has a BS degree in Electrical Engineering and a MSc degree in Physics. He is presently making his Doctoral studies in Porous Media and Thermophysical Properties Laboratory (LMPT) which include the use of lattice gas automata (LGA) for the analysis of single and two-phase flow displacements in 3D porous representations.*

[2] *Paulo C. Philippi is Professor at Federal University of Santa Catarina where he heads the Porous Media and Thermophysical Properties Laboratory (LMPT). He specializes in image analysis and processing, single and multiphase flow in porous media and lattice gas automata (LGA) methods.*

• Corresponding Author (philippi@lmpt.ufsc.br)

[3] *Marcos Cabral Damiani is a software development engineer from the Engineering Simulation and Scientific Software (ESSS) staff. Presently, he is working in the software development of Imago at Porous Media and Thermophysical Properties Laboratory (LMPT).*

1. Introduction

Lattice gas models (LGA) designate a large class of models whose main feature is the presence of a set of particles moving in a discrete space (a lattice). The use of such models to study and simulate fluid dynamics was firstly introduced by J. Hardy, O. de Pazzis e Y. Pomeau[1], in 1973, but it was only after 1986 that these models grow in increased importance due to the work of Frisch et al.[2],[3]. These authors formally demonstrated that the dynamics of such models under certain conditions was described by the Navier-Stokes equations for incompressible flows, and could be used to simulate such flows. Since then, several improvements have been made to simulate multifase flows[4],[5], phase transitions[6], and the development of a new method to simulate fluid dynamics: the Lattice-Boltzmann Method[7],[8].

This work is devoted to present the one-phase lattice gas model, which is applied to estimate the intrinsic permeability of sandstones. The microscopic and macroscopic dynamics are discussed and an order of magnitude analysis is presented to determine the range of applicability of LGA models. Several simulation results are also presented and compared with experimental data.

2. Model

Microscopic Dynamics

Lattice gas models are, basically, composed by particles distributed over a discrete space, the nodes of a regular lattice (Bravais lattice). The particles hop from a site to the neighbor sites in one time step with a discrete and limited velocities set.

Although simulation results presented in this paper are based on the three-dimensional FCHC model[9], the FHP lattice gas model (see fig.1) will be used to exemplify the dynamics and to help understanding the main features of LGA models. This model is based on a hexagonal lattice and is used to simulate 2D flows. Each site in the FHP model has 6 neighbors and it can be populated with 6 moving particles at most, each one with the respective velocity vector $\mathbf{c}_i$, pointing to one neighbor. In addition, a finite number of particles is allowed to be at rest, in each site. Although increasing computational difficulties in the construction of numerical algorithms and resident memory requirements, rest particles are important in LGA models to enlarge the number of possible microscopic states, at each site, and to prevent spurious collision invariants. In present work, one particle is allowed to be at rest, in each site.

In FHP model, the state of a site X at time T is represented by a set of 7 boolean variables, designating the presence (n_i=1) or absence (n_i=0) of a particle in a given direction i, n_0 indicates the presence or absence of a rest particle. For each time step, the dynamic evolution of the model is given in two steps. In the first step, designated as *collision step* (fig. 2), the state of site X is changed following collision rules conceived so as to preserve total mass and momentum of the site. In the second step, called *propagation step* (fig.3), particles are propagated to the neighbor sites, in accordance with their direction at site X after collision step. This is described by the evolution equation:

$$n_i(\mathbf{X}+\mathbf{c}_i, T+1)=n_i(\mathbf{X},T) + \omega_i(n_1,...n_b) \qquad (1)$$

where ω_i: $(n_1,...n_b)\rightarrow\{-1,0,1\}$ represents the collision operator which can take the values –1, 1 or 0, depending on the state $(n_1,...n_b)$ of site X before the collision. Considering S to be the set of 2^b possible states, $s=(s_1,...s_b)$ of site X and α: SXS $\rightarrow$ $\{0,1\}$, to be the transition matrix (with 2^b X2^b elements), the collision operator can be written as

$$\omega_i(n_1,...,n_b) = \sum_s \left[\sum_{s'} \alpha(s,s')(s'_i - s_i) \prod_{j=1}^{b} \delta(n_{j+i}, s_{j+i}) \right] \qquad (2)$$

where s' designates post collision states. In present work, it was considered changes to each possible state s' with the same probability with the inclusion of s between the post collision states.

The FCHC model

Three-dimensional regular lattices do not have the required symmetries and fail in describing fluid flow with isotropic properties. To overcome this problem d'Humières, Lallemand and Frisch[9] proposed the use of the face centered hipercube lattice (FCHC). This lattice is constructed using the vectors:

$$\mathbf{c}_i = perm(\pm 1,\pm 1,0,0) \tag{3}$$

where the symbol "*perm*(a,b,c,d)" indicates all the permutations among a,b,c,d. There are six possible permutations and four combination of signs and, consequently, 24 vectors $\mathbf{c}_i$. Considering the three dimensional projection of FCHC lattice (i. e. the first three dimensions), two kinds of vectors are possible. Twelve vectors have the form

$$\mathbf{c}_i = perm(\pm 1,\pm 1,0) \tag{4}$$

whose moduli are $\sqrt{2}$. These vectors will connect second neighbors in the three dimensional projection.

The remaining twelve vectors have the form

$$\mathbf{c}_i = perm(\pm 1,0,0) \tag{5}$$

correspond to vectors linking the first neighbors in the projection. It is important to notice that each projected vector of this form is the result of the projection of one of the two possible vectors in the four dimensional lattice:

$$\mathbf{c}_i = (perm(\pm 1,0,0),1) \tag{6}$$

and

$$\mathbf{c}_i = (perm(\pm 1,0,0),-1) \tag{7}$$

therefore it is necessary to use two vectors linking the first neighbors in 3D projection, i. e., two particles are allowed to populate each of these directions.

In figure 4 is showed the projection of a 3D face centered cubic lattice in a square lattice.

Forcing the Flow

External body forces **g(X)** may be simulated in LGA by adding a fixed amount of momentum at site X at each unitary time step. In present paper, this is performed after each collision step, by changing n_i by

$$\Delta n_i^g = P(X)\{g_i[n_i(1-n_{i+b/2})-n_{i+b/2}(1-n_i)]+g_{i+b/2}[n_{i+b/2}(1-n_i)-n_i(1-n_{i+b/2})]\} \tag{8}$$

whenever possible, i.e., whenever exclusion principle is not violated and mass is preserved, P(**X**) being 1 when a random variable attributed to **X** is smaller than S(**X**) and 0 otherwise, in accordance with a given probability S(X), related to the external force strength. Eq. (1) is thus, modified, to give:

$$n_i(\mathbf{X}+\mathbf{c}_i, T+1)=n_i(\mathbf{X},T) + \omega_i(n_1,...n_b) + \Delta n_i^g \tag{9}$$

Boltzmann Approximation

Lattice gas simulation starting from a given initial condition may be considered as a single realization of a stochastic process. Considering an *ensemble* of different realizations and calling

$$N_i=<n_i(\mathbf{X},T)> \tag{10}$$

corresponding to the expected value of the boolean variable n_i at a given point X and time T, the evolution equation satisfied by N_i can be found, at a closed form, by supposing that boolean variables n_i at X, T are non-correlated before collision. This is called *molecular chaos* hypothesis and gives

$$N_i(\mathbf{X}+\mathbf{c}_i, T+1) - N_i(\mathbf{X},T) = \Omega_i = \sum_s \left[\sum_{s'} A(s,s')(s'_i - s_i) \prod_{j=1}^{b} \delta(N_{j+i}, s_{j+i}) \right] \quad (11)$$

which is the dynamical evolution equation for the distribution N_i, in the Boltzmann approximation.

In the above equation,

$$\Omega_i = < \omega_i(n_1,...,n_b) > \quad (12)$$

$$A(s, s') = <\alpha(s, s')> \quad (13)$$

Using the semi-detailed balance condition, it may be proved that,

$$\sum_s A(s,s') = 1 \qquad \forall s' \quad (14)$$

Equation (11) has an H-Theorem and an equilibrium solution, which is a Fermi-Dirac distribution function

$$N^o_i = \frac{1}{1+\exp(h+\mathbf{q}.\mathbf{c}_i)} . \quad (15)$$

Due to the discrete nature of the model, a linear low velocity approximation of Eq.(15) is used, written in terms of the density

$$\rho = \sum_{i=1}^{b_m} N_i + N_o b_r , \quad (16)$$

where b_r is the maximum number of rest particles allowed at each site X, and in terms of the mean velocity

$$\mathbf{u} = \frac{1}{\rho} \sum_{i=1}^{b_m} N_i \mathbf{c}_i . \quad (17)$$

This equilibrium solution can be written as

$$N^o_i = f\left[1 + \frac{Db}{c^2 b_m} c_{i\alpha} u_\alpha + \frac{D^2}{2c^4} \frac{b^2}{b_m^2} \left(\frac{1-2f}{1-f} \right) \left(c_{i\alpha} c_{i\beta} - \frac{c^2}{D} (1 - b_r) \delta_{\alpha\beta} \right) u_\alpha u_\beta \right] + O(u^3) \quad (18)$$

for moving particles whereas for rest particles,

$$N^o_o = f\left[1 - \frac{D}{2c^2} \frac{b}{b_m} \left(\frac{1-2f}{1-f} \right) u^2 \right] + O(u^4) \quad (19)$$

In the above equations D is the Euclidean dimension of the lattice, D=2 in FHP and D=4 in FCHC models, $b = b_m + b_r$ and $f = \rho/b$.

Scaling to physical variables

Using h and ε as, respectively, a spatial and a time scale

$$\begin{aligned} \mathbf{x} &= h\mathbf{X} \\ t &= \delta T \end{aligned} \quad (20)$$

x and t may be considered as physical variables, varying continuously in the spatial and time domain of the physical system to be described, when h and δ are small.

Lattice Gas Hydrodynamic Equations

Use of Chapman-Enskog method on the N_i evolution equation, Eq.(6), leads to lattice gas hydrodynamic equations, in the limit of low Knudsen number $Kn = h/L = \delta/\Gamma << 1$, where L is a characteristic length and Γ is a characteristic time:

$$\partial_t(\rho) + \partial_\beta(\rho u_\beta) = 0 \tag{21}$$

$$\partial_t(\rho u_\alpha) + \partial_\beta[g(\rho)\rho u_\alpha u_\beta] = \partial_\alpha(p(\rho, u^2)) + \nu\partial_\beta[\partial_\beta(\rho u_\alpha) + \partial_\alpha(\rho u_\beta)] + \eta\partial_\alpha[\partial_\beta(\rho u_\beta)] \tag{22}$$

where

$$g(\rho) = \frac{2}{3}\left(\frac{1-\rho/12}{1-\rho/24}\right) \tag{23}$$

$$p(\rho, u^2) = c_s{}^2\rho - \frac{5}{4}M^2\rho g(\rho) \tag{24}$$

and $c_s{}^2 = \frac{1}{2}$ is the square of LGA sound speed. The first and the second viscosity coefficients, respectively ν and η, are related to the eigenvalues of collision operator **W.** Equations (21)-(22) differ from Navier-Stokes hydrodynamic equations: i) by the inclusion of a $g(\rho)$ dependence in the inertial term, breaking Galilean invariance, ii) taking M as the Mach number, $M = U/c_s$, by a $O(M^2)$ additional term in the pressure equation (Eq.(24)) and iii) by the inclusion of density ρ *inside* the spatial derivatives in the viscous terms. These *non- physical lattice effects* disappear in the low Reynolds, $Re = U L/\nu$ and Mach numbers, $M = U/c_s$, limits. This was demonstrated by Rothman and Zaleski[10] by using *perturbation analysis*. In the following, a short *order of magnitude analysis* of LGA equations is presented, which corroborates Rothman and Zaleski results.

In fact, Eqs (17)-(18) can be written as

$$\partial_t(\rho) + \rho\partial_\beta(u_\beta) + u_\beta\partial_\beta(\rho) = 0 \tag{25}$$

$$\begin{aligned} r\partial_t(u_a) + u_a\partial_t(r) + rg(r)\partial_b(u_a u_b) + u_a u_b\partial_b[rg(r)] &= \partial_a(p) \\ &+ n\partial_b(r)\left(\partial_b(u_a) + \partial_a(u_b)\right) \\ &+ rn\partial_b\left[\left(\partial_b(u_a) + \partial_a(u_b)\right)\right] \\ &+ n\partial_b\left[\left(u_a\partial_b(r) + u_b\partial_a(r)\right)\right] \\ &+ rh\partial_a\left[\partial_b(u_b)\right] + hu_b\partial_a\left[\partial_b(r)\right] \end{aligned} \tag{26}$$

In the low Mach number limit, viscous effects have the same order of magnitude as the driven force

$$O(\partial_\alpha(p)) = O(\rho\nu\partial_\beta[\partial_\beta(u_\alpha) + \partial_\alpha(u_\beta)]) = \frac{\rho_o U\nu}{L^2} \tag{27}$$

and, in accordance with the state equation, Eq. (24), density fluctuations are related to pressure perturbations by

$$\Delta\rho/\rho_o \sim \frac{\Delta p}{c_s^2\rho_o} \sim \frac{M^2}{Re} \tag{28}$$

For viscous flows the correct time scale to be used is $T_\nu = L^2/\nu$, which is the time scale for the viscous propagation of velocity fluctuations. In this case, in the mass conservation equation, Eq. (21),

$$O(\partial_t(\rho)) = \frac{\Delta\rho U}{L} \sim \frac{\rho_0 c_s}{L}\frac{M^3}{Re} \tag{29}$$

$$O(\rho\partial_\beta(u_\beta)) = \frac{\rho_o U}{L} = \frac{\rho_o c_s}{L}M \tag{30}$$

$$O(u_\beta\partial_\beta(\rho)) = \frac{U\Delta\rho}{L} \sim \frac{c_s\rho_o}{L}\frac{M^3}{Re} \tag{31}$$

and the incompressibility condition

$$\nabla.\mathbf{v} = 0 \tag{32}$$

is recovered in the limit $M^2 << Re$.

A similar analysis carried on the momentum equation, shows that all the terms are of $O\left(\frac{\rho_o U^2}{L}\frac{M^2}{Re}\right)$ excepting the following ones:

$$\rho g(\rho)\partial_\beta\left(u_\alpha u_\beta\right) \sim \frac{\rho_0 U^2}{L} \tag{33}$$

$$\rho\partial_t(u_\alpha) \sim \frac{\rho_o U^2}{L}\frac{1}{Re} \tag{34}$$

$$u_\alpha\partial_t(\rho) \sim \frac{\rho_o U^2}{L}\left(\frac{M}{Re}\right)^2 \tag{35}$$

$$\rho\nu\partial_\beta\left[\left(\partial_\beta(u_\alpha)+\partial_\alpha(u_\beta)\right)\right] \sim \frac{\rho_o U}{L}\frac{1}{Re} \tag{36}$$

and the correct hydrodynamic equations are found when M<<Re<<1:

$$\tilde{n}\partial_t(u_\alpha) = \partial_\alpha(p) + \tilde{n}\acute{i}\partial_\beta\partial_\beta u_\alpha \tag{37}$$

which is the momentum equation for low Reynolds number incompressible flows. It must be observed that, as M<1, the above condition is more restrictive than M^2<<Re<<1.

Boundary conditions

Collision step uses local information only and therefore, boundary conditions are introduced, solely, in the propagation step. In the sites near the wall, all particles that would hit the walls have their velocity reversed, during this step: $\mathbf{c}_i \rightarrow -\mathbf{c}_i$. This is called a *bouncing-back* boundary condition. Bouncing-back restriction leads to non-slip boundary condition at the wall.

In the inlet and outlet regions periodic boundary conditions are used: every particle exiting the simulation region from one edge is injected into the other edge with the same velocity. In the simulations of flows through porous media non-solid regions were added in the inlet and the outlet boundaries in order to guarantee that a particle exiting the lattice will never encounters a wall in the other edge. These non-solid region were also used to force the flow in the interested region, acting as hydraulic pumps to compensate head loss produced by porous structure

3. Validation: Poiseuille flow

Navier-Stokes equations predict a parabolic velocity profile for the flow between two parallel plates. Figure 5 shows simulation results compared with theoretical one. Simulation was performed using FCHC model, in a three-dimensional channel, with 39 lattice-units in thickness and periodic conditions were imposed in the outer plane. As can be seen, a good agreement between the simulated and the theoretical results was obtained.

4. Results

Several simulations were performed to calculate intrinsic permeability of Brazilian sandstones. Simulations start from three-dimensional representations of the porous structure, reconstructed from petrographic thin plates by using Liang *et al*. method[11],[12]. Details about reconstruction method can be found in a companion paper submitted to present meeting[12]. Segmentation methods provide binary two-dimensional images, from digital color and/or gray-level images. Three-dimensional reconstruction is based on the generation of three-dimensional stochastic realizations, preserving the statistical moments of phase function, which are measured on the target binary image. Present reconstruction method preserves the two first moments of the phase function: porosity and auto-correlation. A main reconstruction parameter is the sampling factor ‘n’. Sampling factor n=1 means that three-dimensional representation and the binary image have the

same spatial resolution. As sampling factor n increases, resolution decays with the same ratio. In general, it is very difficult to preserve original resolution, in reconstructed representations, due to limitations inherent to the reconstruction method itself, which fails in preserving the fine details of the porous structure. In this sense, the best reconstructed microstructure is considered to be the one generated with the sampling factor that gave the best agreement between pore size distributions, measured on the original binary image and on cross-sections of the three-dimensional representation. Further details can be found in references [11]-[13]. Figure 6 gives a comparison for pore size distribution between reconstructed three-dimensional representations and original binary image for brazilian sandstone P26.2K69.7 (source data from CENPES/Petrobras). Best sampling factor is n=2. The volume amount of small features is overestimated in reconstructed representations with n=1, whereas this amount is underestimated for n=3.

Table I gives some simulation results and comparison with experimental data for Brazilian sandstones. Best sampling factor is indicated by an (*). Another important reconstruction parameter is the 3D representation linear size N. Size N must be great enough to assure statistical homogeneity, with respect to fluid flow problem. Nevertheless, computer resident memory requirements are multiplied by 8, when N doubles. In this way, considering computer limitations, simulation starts from small and proceeds to larger linear sizes until convergence.

A typical simulation in a structure of 100^3 voxels uses approximately three hours, using a Pentium II - 300MHz microcomputer and ten hours to simulate in a structure of 200^3

5. Conclusions

A lattice gas model was presented as a tool for performing fluid dynamic simulations in complex geometry, especially in porous media. The macroscopic behavior of the model was discussed in order to find its range of applicability. Finally, simulation results were presented, in the calculation of the intrinsic permeability of Brazilian sandstones.

Results appear to confirm the suitability of LGA based methods in the calculation of intrinsic permeability.

Acknowledgements

The authors would like to acknowledgeCENPES/PETROBRAS (Centro de Pesquisas e Desenvolvimento Leopoldo A. Miguez de Mello) for providing the images and experimental data for Berea and Brazilian sandstones and the financial support of CNPq (Conselho Nacional de Desenvolvimento Científico e Tecnológico), PADCT (Programa de Apoio ao Desenvolvimnto Científico e Tecnológico), RHAE (Programa de Formação de Recursos Humanos em Areas Estratégicas) and FINEP (Financiadora de Estudos e projetos).

7. References

[1] – Hardy, J., Pomeau, Y., de Pazzis O. (1973). “Time Evolution of a Two-Dimensional Model System. I. Invariant States and Time Correlation Functions” *J. Math. Phys.* **14,** 1746-1759.

[2] – Frisch, U., Hasslacher B., Pomeau Y. (1986). “Lattice-Gas Automata for the Navier-Stokes Equation” *Physical Review Letters* **56**, 1505-1508.

[3] – Frisch, U., d’Humières, D., Hasslacher, B., Lallemand, P., Pomeau, Y. and Rivet, J. (1987). “Lattice Gas Hydrodynamics in Two and Three Dimensions” *Complex Systems* **1**, 649-707.

[4] – Rothmann, D. H., Keller, J. M. (1988). “Immiscible Cellular-Automaton Fluids” *J. Stat. Phys.* **52**, 1119-1127.

[5] – Chen, S., Doolen G. D., Eggert, K., Grunau, D. and Loh, E. Y. (1991). “Local lattice-gas model for immiscible fluids” *Physical Review A* **43,** 7053-7056.

[6] – Appert, C. and Zaleski (1990). “A lattice gas liquid-gas transition” *Physical Review Letters* **64**, 1-4.

[7] - McNamara G. G. and Zanetti G. (1988). “Use of the Boltzmann Equation to Simulate Lattice-Gas Automata” *Physical Review Letters* **61**, 2332-2335.

[8] – Higera, F. and Jimenez, J. (1989). “Boltzmann approach to lattice gas simulations.” *Europhys. Lett.* **9**, 663-668.

[9] – d’Humières, D., Lallemand, P., and Frisch, U. (1986). “Lattice gas models for 3D hydrodynamics” *Europhys. Lett.* **2**, 291-297.

[10] – Rothman, D. H., Zaleski, S. (1997). *Lattice-gas cellular automata: simple models of complex hydrodynamics* (Cambridge University Press).

[11] – Liang, Z. R.. (1997) “Computer Generation and Aplication of 3-D Reconstructed Porous Structures: From 2-D Images to the Prediction of Permeability” Doctoral Thesis Depto de Eng. Mecânica, UFSC.

[12] – Liang, Z. R., Fernandes, C. P., Magnani, F.S. and Philippi, P. C., (1998) “A Reconstruction Technique of 3-D Porous Media by using Image Analysis and Using Fourier Transform”, *Journal of Petroleum Science and Engineering***, 21**, 3-4, 273-283.

[13] – M. C. Damiani, C. P. Fernandes, A. D. Bueno, L. O. E. Santos, J. A. B. da Cunha Neto, P. C. Philippi “Predicting Physical Properties of Reservoir Rocks from the Microstructural Analysis of Petrographic Thin Sections”. Submitted to Produccion 2000 / Aplicaciones de la ciencia en la ingeniería de petróleo**, May 08-12 /2000, Foz de Iguaçu**

Figures and Tables

Sandstone Sample	Experimental Permeability	Reconstructed Image Linear Size (N)	Sampling Factor (n)	Simulated Permeability
67409	441	100	6	469
67409	441	100	5 (*)	368
67409	441	200	5 (*)	462
59853	145	150	3	218
59853	145	100	4 (*)	238
59853	145	150	4 (*)	256
P26.2K69.7	69.7	150	2 (*)	90
P26.2K69.7	69.7	200	2 (*)	77
51446	154	100	4	55
51446	154	100	5	64
51446	154	100	6 (*)	81
51440	316	100	4	261
51440	316	100	5	238
51440	316	100	6 (*)	316

(*) Best sampling factor

Table I - Simulation results and comparison with experimental data (Experimental data and source digital images where furnished by CENPES/ Petrobras)

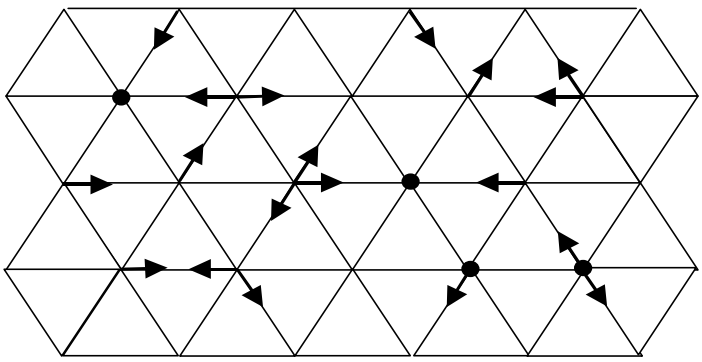

Figure 1: FHP model. The arrows represent the moving particles and the circles represent the rest particles.

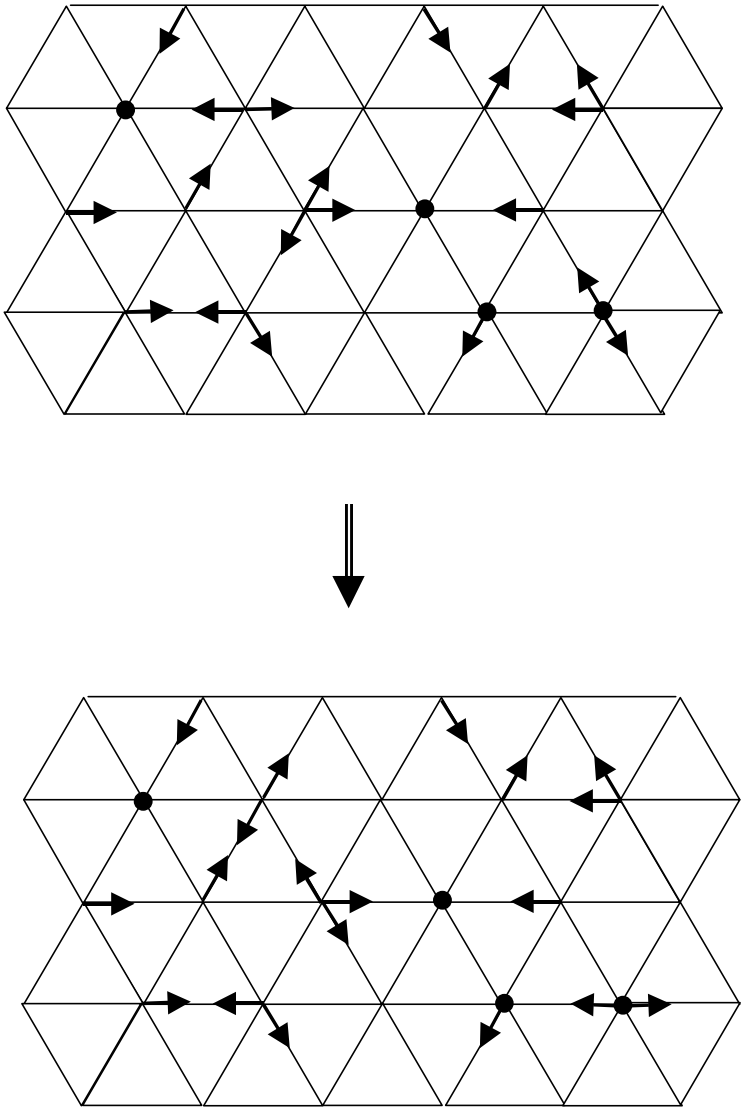

Figure 2: Effect of collisions for a given configuration of the FHP model

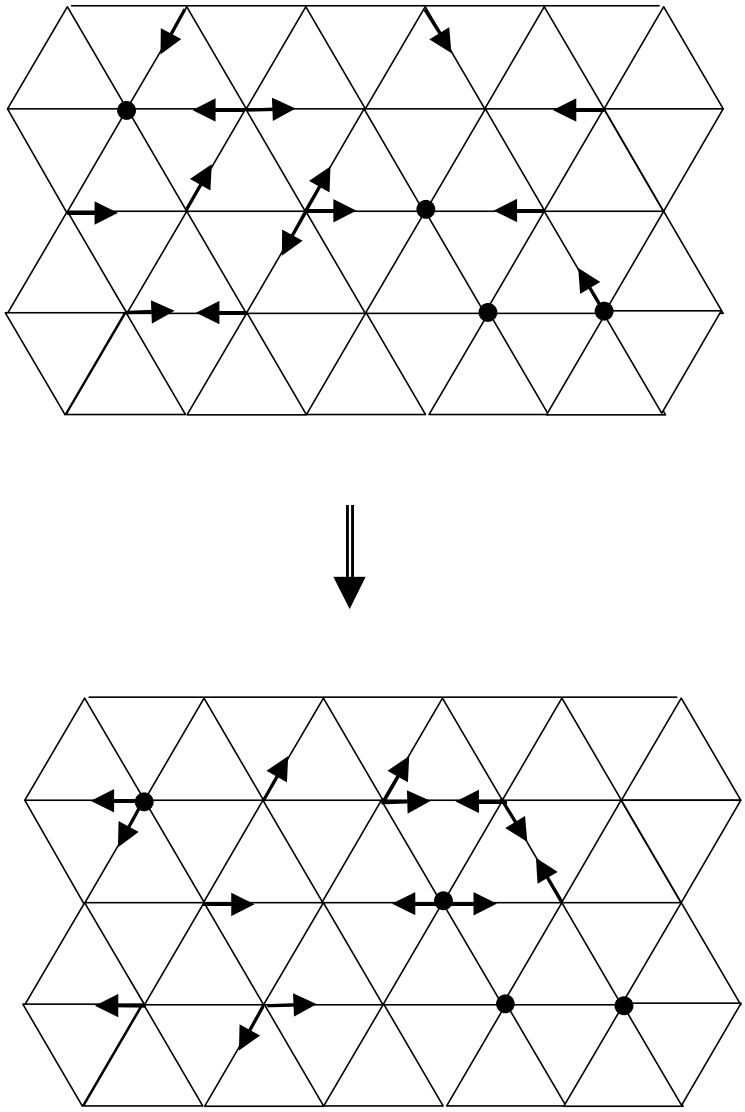

Figure 3: Effect of propagation for a given configuration of the FHP model

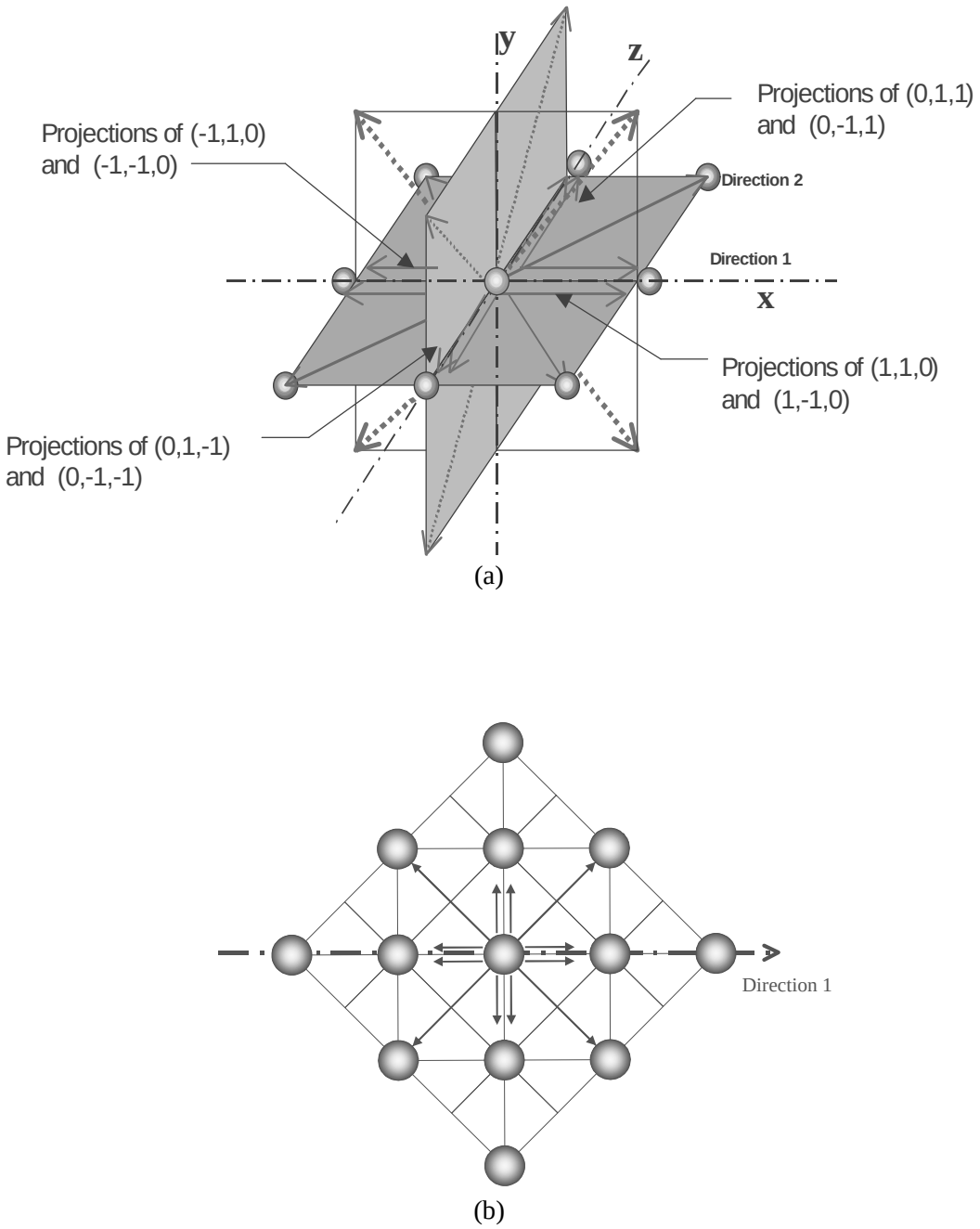

Figure 4. (a) Projection of a three-dimensional lattice whose elemental vectors are given by perm (±1,±1,0) on the plane xz. Microscopic states are given by (s_{11},s_{12},s_2,s_{31},s_{32},s_4,s_{51},s_{52},s_6,,s_{71},s_{72}, s_8). When s_{11} and s_{12} are both equal to 1, before the propagation step, *two particles* are to be propagated from site X to its neighbor site in direction 1, resulting from the projections of directions (1.1.0) and (1, -1, 0). Vectors c_i have all the same norm $\sqrt{2}$, when lattice unit is considered to be unitary. In this way, each site has 8 neighbors in the plane xz, composing a regular plane lattice where the state of each site is represented by a vector with 12 Boolean variables representing moving particles.(b) Plane xz, showing the main axes neighbors to site X. Each of these sites can exchange two particles with central site.

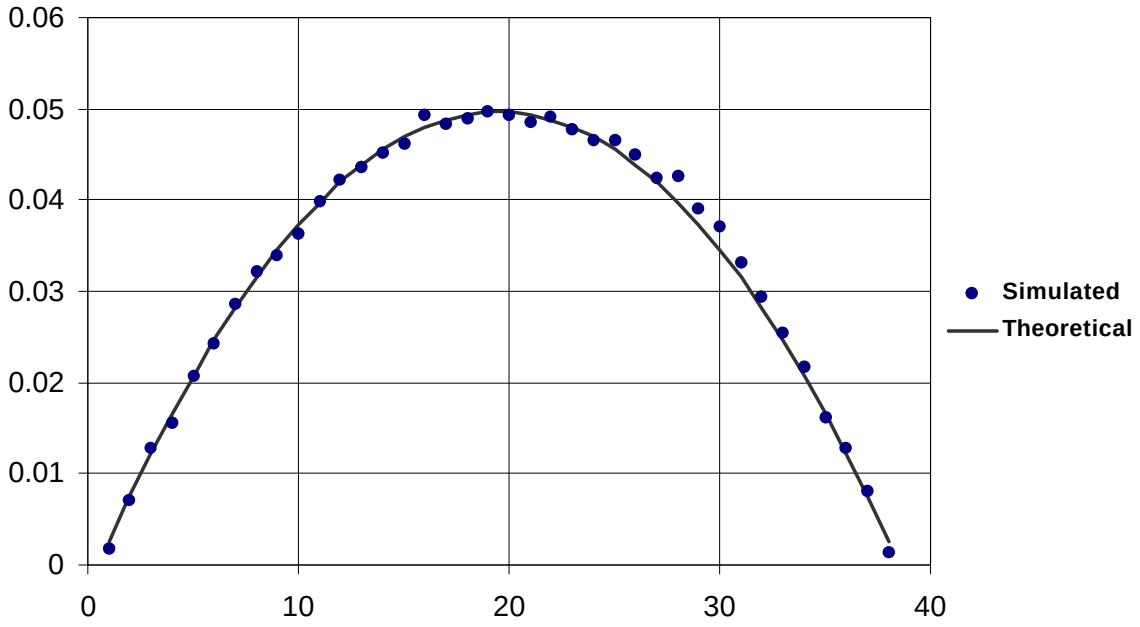

Figure 5. Velocity profile of a flow between two parallel plates. Simulation was performed using a lattice of 40 sites in the direction perpendicular to flow plane. Periodic conditions were used.

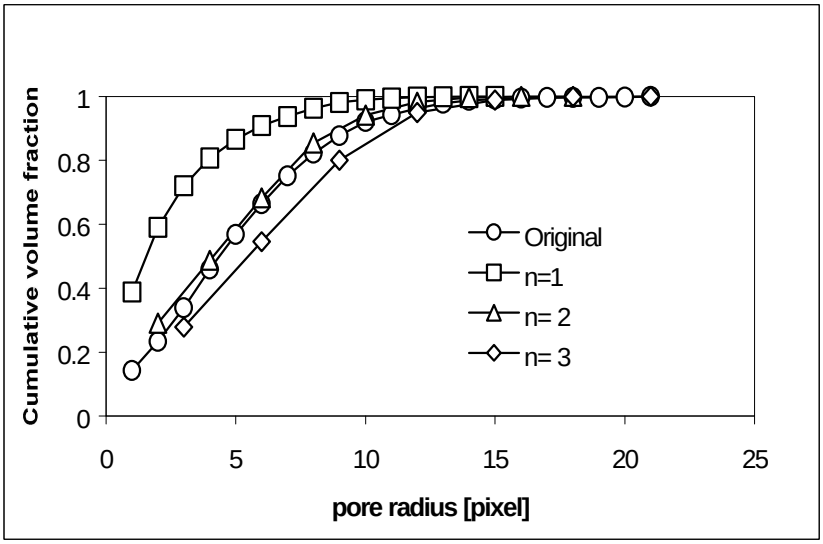

Figure 6 Comparison for pore size distribution between reconstructed three-dimensional representations and original binary image for brazilian sandstone P26.2K69.7 (Digital images where